Nano Energy (2012) 1, 466–471

Available online at www.sciencedirect.com

SciVerse ScienceDirect

journal homepage: www.elsevier.com/locate/nanoenergy

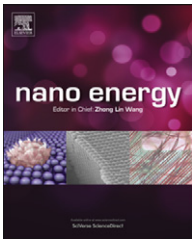

RAPID COMMUNICATION

Self-assembled nanoporous rutile TiO_2 mesocrystals with tunable morphologies for high rate lithium-ion batteries

Zhensheng Hong[a], Mingdeng Wei[a,*], Tongbin Lan[a], Guozhong Cao[b,*]

[a]*Institute of New Energy Technology and Nano-Materials, Fuzhou University, Fuzhou, Fujian 350002, China*
[b]*Department of Materials Science and Engineering, University of Washington, 302M Roberts Hall, Seattle, WA 98195, USA*

Received 21 January 2012; received in revised form 25 February 2012; accepted 25 February 2012
Available online 4 March 2012

KEYWORDS
Mesocrystal;
Rutile TiO_2;
Self-assembly;
High rate;
Lithium-ion battery

Abstract
Wulff-shaped and nanorod-like nanoporous mesocrystals constructed from ultrathin rutile TiO_2 nanowires were successfully fabricated for the first time in the presence of the surfactant sodium dodecyl benzene sulfonate (SDBS). SDBS played a key role in the homoepitaxial self-assembly process, in which titanate nanowires were used as the primary building blocks for forming mesocrystals accompanying with a simultaneous phase transition. The nanoporous rutile TiO_2 mesocrystals have a large surface area and were subjected to detailed structural characterization by means of X-ray diffraction (XRD), scanning and transmission electron microscopy (SEM/TEM) including high-resolution TEM (HRTEM) and selected area electron diffraction (SAED). Furthermore, the nanoporous rutile TiO_2 mesocrystals were applied as the electrode materials in rechargeable lithium-ion batteries and demonstrated a large reversible charge–discharge capacity, excellent cycling stability and high rate performance. These properties were attributed to the intrinsic characteristic of the mesoscopic structured TiO_2 with nanoporous nature and larger surface area (which favored fast Li-ion transport), as well as the presence of sufficient void space to accommodate the volume change.

Introduction

Mesocrystals as proposed by Cölfen et al. [1–3] are 3D ordered superstructures, with potential new physical and chemical properties arising from their unique mesostructure. Such specific morphologies—consisting of a few to many thousand primary units (of size 1–1000 nm) assembled in an orderly fashion—were first reported in biominerals, such as corals, sea urchins and nacres [4–6]. It is worth mentioning that mesocrystals are from via a so-called ‘‘non-classical crystallization’’, which involves the mesoscopic transformation of self-assembled and metastable precursor particles into a single nanoparticulate superstructure [1,7].

*Corresponding authors.
E-mail addresses: wei-mingdeng@fzu.edu.cn (M. Wei), gzcao@u.washington.edu (G. Cao).

2211-2855/$ - see front matter © 2012 Elsevier Ltd. All rights reserved.
doi:10.1016/j.nanoen.2012.02.009

In this process, organic additives are generally used to stabilize the primary nanoparticles, and to direct their self-assembly into a mesocrystal [1,3,7]. It should be noted that biominerals are highly evolutionarily optimized materials, which indicate that non-classical crystallization is a favorable crystallization route that has the potential to be applied in the synthesis of functional materials with advanced properties. In fact, mesocrystals have recently been applied to functional metal oxides such as TiO_2 [8–14], ZnO [15], $BiVO_4$ [16], and $LiFePO_4$ [17], producing improved properties. Specific electrode materials fabricated using hierarchical and porous mesocrystals can be considered as ideal materials for high-performance Li-ion insertion [3,18]. TiO_2 has been considered as a potential anode for lithium-ion batteries (LIBs) due to its intrinsic advantages in safety, low cost, and good cyclic stability [19]. However, one drawback is that the poor lithium-ion and electronic conductivity of bulk TiO_2 polymorphs limit their performance at high charge/discharge rates. To overcome this obstacle, nanostructured and porous TiO_2 has been developed and applied as electrode materials for LIBs. For example nanometer-sized rutile TiO_2 exhibited a much higher electroactivity towards Li insertion than micrometer-sized rutile TiO_2 [20]. Nano- or meso-porous TiO_2 materials have been shown to be promising high rate anode materials [12,21,22]. It is notable that the performance of TiO_2 depends largely on its crystalline phase, size, surface state and microstructures [23,24]. TiO_2 mesocrystals with the desired crystal phases, intrinsic porous structures, and tunable architectures would offer the potential for significantly enhanced Li-ion insertion performance. Although the anatase TiO_2 mesocrystals have been widely reported [8–12], rutile TiO_2 mesocrystals are relatively rare [13,14,25] and nanoporous rutile TiO_2 mesocrystals have never been prepared and used as anode materials for LIBs. In the present work, we first report the self-assembled synthesis of unique nanoporous rutile TiO_2 mesocrystals with much larger surface area than that reported in the literatures [13,14,25]. The mesocrystals with micropores and mesopores coexisting were constructed from ultrathin nanowires, and the tunable morphology (from Wulff-shape to nanorod-like) was directed using sodium dodecyl benzene sulfonate (SDBS). It was found that the assembly process of the nanoporous rutile TiO_2 mesocrystals (different morphologies) and a simultaneous phase transition from titanate to rutile TiO_2. Furthermore, the nanoporous rutile TiO_2 mesocrystals were applied as electrode materials for Li-ion insertion; they exhibited a large reversible lithium-ion charge–discharge capacity, excellent cyclic stability and high rate performance.

Experimental

Synthesis and characterizations

The nanoporous TiO_2 mesocrystals were prepared through two sequential steps: first titanate nanowires were synthesized by means of hydrothermal growth in highly basic aqueous solution and acid-washed, and then titanate nanowires dispersed in acidic aqueous solution were allowed to assemble into different morphology in the presence of SDBS. Synthesis of titanate nanowires is similar to the process reported in our previous work [25]. Typically, 1 g of TiO_2 (anatase) was dispersed in a 50 mL of 15 M aqueous KOH solution. After stirring for 10 min, the resulting suspension was transferred into a Teflon-lined stainless steel autoclave with a capacity of 75 mL. The autoclave was kept at 170 °C for 72 h and then cooled to room temperature. The resulting precipitate was washed with 0.1 M HNO_3 solution until pH value of 1–2 was reached. The final product was then collected by centrifugation and dried at 70 °C for 12 h in air. Synthesis of nanoporous TiO_2 mesocrystals started with dispersing 150 mg of precursor titanate nanowires (0.2 mmol) and sodium dodecyl benzene sulfonate (SDBS) (the molar ratio of titanate:SDBS is from 0.09 to 0.15) in 50 mL of HNO_3 (2 M) solution under stirring at 70 °C for 7 days, and the final product was obtained by centrifugation, washed with distilled water and ethanol several times, dried at 60 °C overnight, and then calcined at 400 °C for 2 h.

Scanning electron microscopy (SEM, S4800 instrument) and Transmission electron microscopy (TEM, FEI F20 S-TWIN instrument) were applied for the structural characterization of the resulting titanate nanowires and mesocrystals. X-ray diffraction (XRD) patterns were recorded on a PANalytical X'Pert spectrometer using the Co Kα radiation (λ=1.78897 Å), and the data were changed to Cu Kα data. N_2 adsorption–desorption analysis was measured on a Micro-meritics ASAP 2020 instrument (Micromeritics, Norcross, GA, USA). The pore size distributions of the as-prepared samples were analyzed using the Barrett Joyner Halenda (BJH) method.

Electrochemical measurements

For the electrochemical measurement of Li-ion intercalation, nanoporous TiO_2 mesocrystals were admixed with polyvinylidene fluoride (PVDF) binder and acetylene black carbon additive in a weight ratio of 70:20:10, following a standard method as widely used in literature [26]. The mixture was spread and pressed on copper foil circular flakes as working electrodes (WE), and dried at 120 °C in vacuum for 12 h. Lithium foils were used as the counter electrodes. The electrolyte was 1 M $LiPF_6$ in a 1/1/1 (volume ratio) mixture of ethylene carbonate (EC), ethylene methyl carbonate (EMC) and dimethyl carbonate (DMC). The separator was UP 3093 (Japan) micro-porous polypropylene membrane. The cells were assembled in a glove box filled with highly pure argon gas (O_2 and H_2O levels $<$1 ppm), and charge/discharge tests were performed in the voltage range of 1–3 V (Li^+/Li) at different current densities on a Land automatic batteries tester (Land CT 2001A, Wuhan, China).

Results and discussion

Pure rutile TiO_2 mesocrystals, as evidenced by XRD patterns shown in Fig. S1, were prepared using hydrogen titanate nanowires as a precursor (with TEM and HRTEM shown in Fig. S2) in a HNO_3 solution under the mild condition in the presence of SDBS with subsequent calcination (performed at 400 °C for 2 h). Fig. 1(a–b) shows SEM images of rutile TiO_2 mesocrystals obtained in the presence of SDBS (the molar ratio of titanate/SDBS is 0.09), Wulff-shaped, uniform octahedral rutile TiO_2 was observed with a particle size of

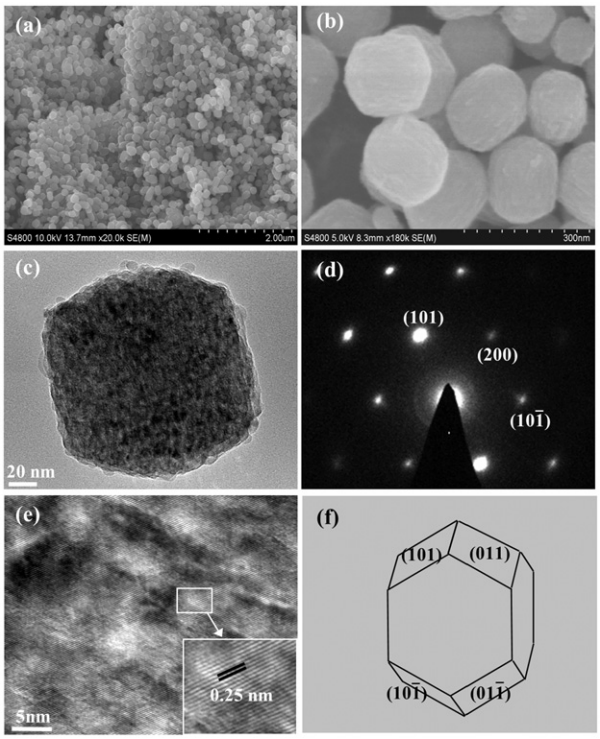

Figure 1 Rutile TiO_2 mesocrystals obtained in the presence of SDBS (the molar ratio of titanate/SDBS is 0.09): (a, b) low and high magnification SEM images, (c, e) TEM image and HRTEM images, (d) corresponding SAED pattern, and (f) is a structural illustration of Wulff shape for rutile TiO_2.

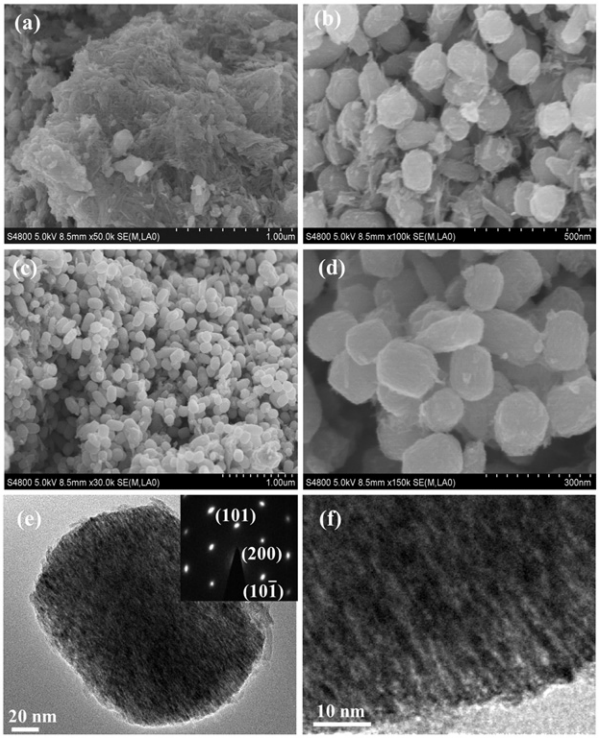

Figure 2 SEM images (a–d) and TEM images (e, f) of the samples obtained in the presence of SDBS (the molar ratio of titanate/SDBS is 0.09) under the different reaction times: (a) 1, (b) 3, (c–f) 5 days. The inset in (e) is the related SAED pattern of the whole mesoparticles.

100–300 nm (~200 nm on average). A rough surface was clearly observed in the high magnification SEM image, suggesting that the obtained particles were not classic single crystals. Fig. 1(c) shows a typical TEM image of a single mesocrystal, confirming that the particles were composed of nanosized subunits. The related selected area electron diffraction (SAED) pattern (shown in Fig. 1d) exhibited "single-crystal-like" diffraction spots corresponding to rutile TiO_2, indicating that a mesocrystal structure was formed. The diffraction spots were slightly elongated, suggesting that there was a small lattice mismatch in the assembly in the same orientation, which is typical of mesocrystals [1,3]. Fig. 1(e) shows an HRTEM image of a mesocrystal, the porous nature of the Wulff-shaped rutile TiO_2 mesocrystals is clearly revealed. The lattice fringe was found to be approximately 0.25 nm (Fig. 1(e), inset), corresponding to d_{101} spacing of rutile TiO_2 crystal. The porous structure of the obtained mesocrystals (as observed in the HRTEM image), showed similarities with the structure of porous zeolite crystals. According to the literature, such porous single crystals are typical for mesocrystals formed through an oriented self-assembly process in which the links between nanocrystals are formed partly by the nanocrystals themselves and partly by an organic substance [1,6].

To investigate the formation mechanism of rutile TiO_2 mesocrystals with Wulff shape, a series of samples were harvested at different reaction time intervals without calcinations. These samples were then carefully characterized using SEM and TEM, and the results are shown in Fig. 2. As shown in Fig. 2(a), numerous nanowires were clearly observed when the reaction was performed for 1 day. After the reaction time was increased to 3 days, a large number of nanowires aggregates appeared, in addition to the residual dispersed nanowires (see Fig. 2b). Fig. 2(c–d) shows SEM and high magnification SEM images of the products obtained after 5 days; uniform mesocrystals with a Wulff shape were basically formed besides partly imperfect adjacence. Fig. 2(e) shows a typical TEM image of a single mesocrystal, confirming that it is composed of nanowire subunits. The HRTEM image in Fig. 2(f) reveals that the nanowire subunits were about 3–5 nm in diameter. The SAED pattern depicted in the inset of Fig. 2(e) suggests that the TiO_2 mesocrystals with Wulff shape actually exhibited a single-crystal-like mesoscopic structure. HRTEM and SAED data collected for the sample after 7 days also confirmed that the obtained mesocrystals were arranged along the [101] direction (see Fig. S3). In addition, the phase transition from titanate to rutile TiO_2 was achieved gradually with increasing reaction time, as shown in the XRD patterns (Fig. S4).

It was expected that the morphology of the mesocrystals could be controlled simply by adjusting the concentration of the SDBS; this was confirmed by the images shown in Fig. 3. As shown in Fig. 3(a–b), nanorod-like mesocrystals about 250–400 nm in length and 60–100 nm in diameter were obtained in the presence of SDBS (the molar ratio of titanate/SDBS is 0.15). When the molar ratio was decreased to 0.11, mesocrystals with Wulff shape appeared, as depicted in Fig. 3(c). Fig. 3(d) shows a TEM image of the sample synthesized in the presence of SDBS (the molar ratio

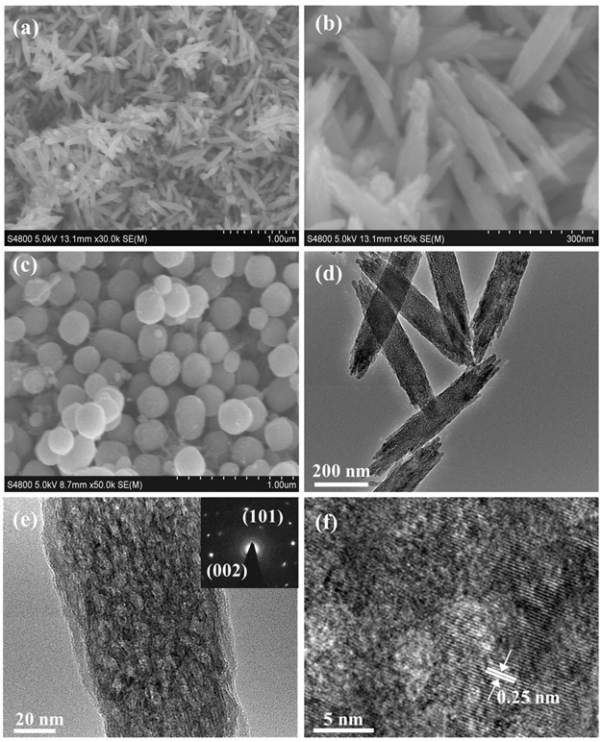

Figure 3 SEM images (a-c), TEM (d) and HRTEM (e, f) images of the samples obtained in the presence of SDBS with different molar ratio of titanate/SDBS: (a-b, e-f) 0.15 and (c) 0.11. The inset in (e) is SAED pattern.

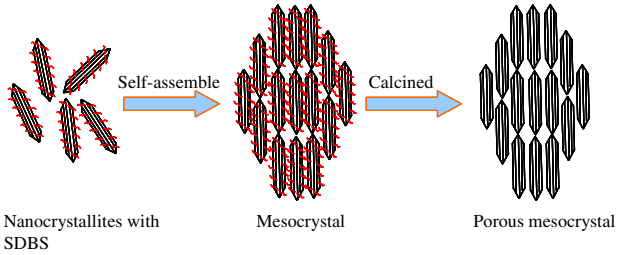

Scheme 1 Schematic of a tentative mechanism for the formation of rutile TiO_2 mesocrystals.

of titanate/SDBS is 0.11). This image confirmed that the nanorod-like mesocrystals were also made up of nanowires units. The porous nature of the mesocrystals can be observed in the HRTEM images presented in Fig. 3(d-e). The related SAED pattern (shown in the inset of Fig. 3d) also confirmed a single-crystal-like structure in the nanorod-like mesocrystals. Additives are usually needed in the synthesis of mesocrystals [1,3]. Herein, we have reported the first tunable synthesis of mesocrystals using SDBS as a surfactant, and have found that rutile TiO_2 mesocrystals with different morphologies can be easily produced simply by adjusting the concentration of SDBS.

To confirm the porous nature of the TiO_2 mesocrystals, N_2 adsorption-desorption isotherms were measured, as shown in Fig. S5. These data indicated that micropores and mesopores coexist in the mesocrystals with nanorod-like and Wulff shape. The Brunauer-Emmett-Teller (BET) surface area for the former was approximately 89.6 m^2g^{-1}, while for the latter it was found to be ca. 135.5 m^2g^{-1}. It was found that the mesopore volumes were very similar for the different types of mesocrystals (0.12 m^3g^{-1}). However, the micropore volume of the Wulff-shaped mesocrystals (0.027 m^3g^{-1}) was much larger than that of the nanorod-like mesocrystals (0.017 m^3g^{-1}), indicating that the number of micropores inside Wulff-shaped mesocrystals was much larger than in the nanorod-like mesocrystals. Pore size distributions ranging from 0.5 to 1.4 nm was calculated by the Horváth-Kawazoe method, as shown in the insets of Fig. S5.

A tentative mechanism was proposed for the formation of porous rutile TiO_2 mesocrystals (as shown in Scheme 1), based on the experimental results. The proposed mechanism is similar to the typical formation of a mesocrystal as described by Cölfen et al. [1,3] The mesocrystals were formed through the homoepitaxial self-assembly of nanocrystallites, with a SDBS additive. In the present reaction, the presence of the additive would hinder the diffusion of the nanocrystals, allowing their attachment and assembly into ordered aggregates (mesocrystals) to occur at a lower energy state. Porous mesocrystals with mesoporous and microporous nature (Fig. S6) would then be obtained after the removal of the organic substance (Fig. S7). It is notable that the morphology of the mesocrystals significantly depended on the content of the SDBS additive, and ultimately led to the formation of Wulff-shaped rutile mesocrystals. It is pointed out that the organic additive could be in favor of lowering the surface energy of the primary nanocrystals and the mesocrystal is an intermediate of the single crystal [1,3]. Therefore, it could be understood that the nanocrystal subunits were likely to assemble into the Wulff-shaped rutile mesocrystals in the presence of enough content of additives, corresponding to the principle of the growth of single crystal [27].

Recently, a great deal of attention has been focused on the use of nanostructured rutile TiO_2 for electrode materials in LIBs [20,28-31]. The nanoporous rutile TiO_2 mesocrystals synthesized in this study offer a much larger specific surface area and a shorter transport distance, and thus should promise better lithium-ion insertion properties. Fig. 4(a) shows the charge-discharge profiles of the rutile TiO_2 mesocrystals with Wulff shape at a current density of 1 C (1 C=170 mAg^{-1}), for the initial two cycles over the potentials of 1.0-3.0 V. A large capacity of 312.3 $mAhg^{-1}$ was obtained at the first discharge, higher than that of previously reported nanosized rutile TiO_2 [20] as well as mesoporous rutile TiO_2 constructed with rod-like nanocrystals as building blocks [28]. A voltage plateau near 1.05 V was observed in the first discharge curve, which can be attributed to the irreversible change in the structure of the rutile TiO_2 upon deeper Li-ion insertion [20]. The sloped discharge curve in the second cycle might be ascribed to the irreversible formation of a 'nanocomposite' consisting of crystalline grains and amorphous regions [32-34]. Fig. 4(b) shows the rate capability of the rutile TiO_2 mesocrystals with Wulff shape from 0.2 to 20 C, for 10 cycles at each current rate. Large capacities of 397.9 and 275.6 $mAhg^{-1}$ were obtained with the first discharge and charge cycle at a current density of 0.2 C; this might be attributed to the fact that the nanoporous mesocrystals had a large surface area, and could

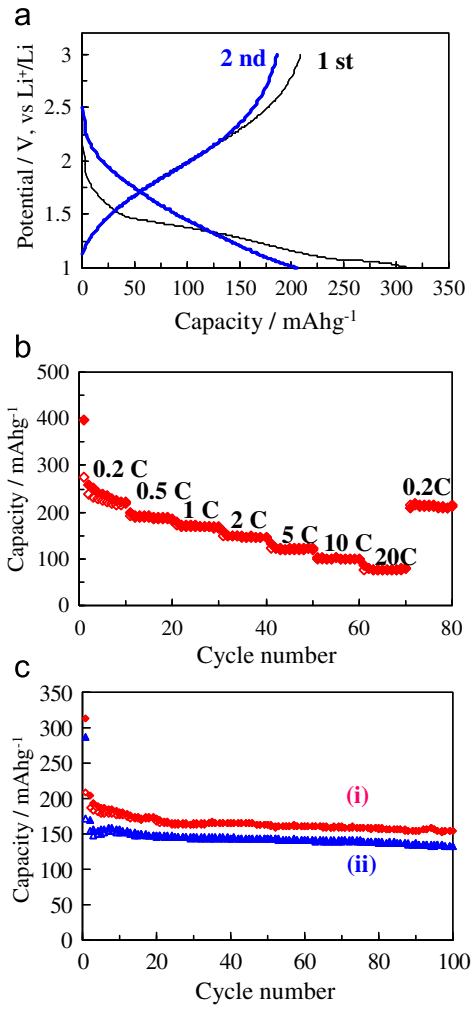

Figure 4 (a) Charge–discharge profiles at a current density of 1 C and (b) rate capability from 0.2 to 20 C of rutile TiO_2 mesocrystals with Wulff shape; (c) cycling performance at a constant current density of 1 C for rutile TiO_2 mesocrystals with different morphologies: (i) Wulff shape, and (ii) nanorod-like.

provide more sites for lithium insertion. It was also revealed that the mesocrystal electrode retained a good rate capability even if the current rate was increased from 0.2 to 20 C. Remarkably, a capacity of 76.5 $mAhg^{-1}$ could be delivered at current rates as high as 20 C; a large capacity of 216 $mAhg^{-1}$ could be regained when the current rate was lowered again to 0.2 C. Fig. 4(c) presents the cycling behavior of the rutile TiO_2 mesocrystals with different morphologies, at a current rate of 1 C. It clearly shows that both of the rutile TiO_2 mesocrystals exhibited excellent cycling stability. Capacities of 154 and 133 $mAhg^{-1}$ could be retained after 100 cycles for the Wulff-shaped and nanorod-like TiO_2 mesocrystals, respectively. The electrochemical properties of the Wulff shaped TiO_2 mesocrystals were significantly and clearly better than those of the nanorod-like mesocrystals; this might be ascribed to the larger surface area arising from the larger number of micropores in the former. The nanoporous and large-surface-area nature of the rutile mesocrystals facilitated their contact with the electrolyte, and hence favored fast Li-ion transport. These factors—along with the sufficient void space accommodating volume change—resulted in the large capacity and high rate performance.

Conclusions

Unique nanoporous mesocrystals, constructed from ultrathin rutile TiO_2 nanowires and with Wulff-shaped and nanorod-like morphologies, were successfully fabricated for the first time in the presence of SDBS. It was revealed that the SDBS played a key role during the homoepitaxial self-assembly process, which involved the aggregation of the precursor titanate nanowires (acting as the primary building blocks) and a simultaneous phase transition from precursor titanate to rutile TiO_2. These nanoporous rutile TiO_2 mesocrystals were used as the electrode materials in rechargeable lithium-ion batteries for the first time; they demonstrated a large reversible charge–discharge capacity, excellent cycling stability and high rate performance. These properties were attributed to the intrinsic nanoporous and large surface area characteristics of the mesoscopic structured TiO_2.

Acknowledgments

This work was financially supported by the National Science Foundation of China (NSFC 21173049 and 21073039), the Fujian Province Fund (JA10016) and the Key Laboratory of Novel Thin Film Solar Cells, CAS.

Appendix A. Supporting information

Supplementary data associated with this article can be found in the online version at doi:10.1016/j.nanoen.2012.02.009.

References

[1] H. Cölfen, M. Antonietti, Angewandte Chemie International Edition 44 (2005) 5576–5591.
[2] S.H. Yu, H. Cölfen, K. Tauer, M. Antonietti, Nature Materials 4 (2005) 51–55.
[3] R.Q. Song, H. Cölfen, Advanced Materials 22 (2010) 1301–1330.
[4] S. Mann, Nature 365 (1993) 499–505.
[5] L. Addadi, S. Weiner, Angewandte Chemie International Edition 31 (1992) 153–169.
[6] L. Zhou, P. O'Brien, Small 4 (2008) 1566–1574.
[7] M. Niederberger, H. Colfen, Physical Chemistry Chemical Physics 8 (2006) 3271–3287.
[8] L. Zhou, D. Smyth Boyle, P. O'Brien, Chemical Communications (2007) 144–146.
[9] L. Zhou, D. Smyth-Boyle, P. O'Brien, Journal of the American Chemical Society 130 (2008) 1309–1320.
[10] J. Feng, M. Yin, Z. Wang, S. Yan, L. Wan, Z. Li, Z. Zou, CrystEngComm 12 (2010) 3425–3429.
[11] R.O. Da Silva, R.H. Goncalves, D.G. Stroppa, A.J. Ramirez, E.R. Leite, Nanoscale 3 (2011) 1910.
[12] J. Ye, W. Liu, J. Cai, S. Chen, X. Zhao, H. Zhou, L. Qi, Journal of the American Chemical Society 133 (2011) 933–940.
[13] S.-J. Liu, J.-Y. Gong, B. Hu, S.-H. Yu, Crystal Growth & Design 9 (2009) 203–209.

[14] D. Zhang, G. Li, F. Wang, J.C. Yu, CrystEngComm 12 (2010) 1759–1763.
[15] Z. Li, A. Gessner, J.-P. Richters, J. Kalden, T. Voss, C. Kübel, A. Taubert, Advanced Materials 20 (2008) 1279–1285.
[16] L. Zhou, W. Wang, L. Zhang, H. Xu, W. Zhu, Journal of Physical Chemistry C 111 (2007) 13659–13664.
[17] J. Popovic, R. Demir-Cakan, J. Tornow, M. Morcrette, D.S. Su, R. Schlögl, M. Antonietti, M.-M. Titirici, Small 7 (2011) 1127–1135.
[18] A. Magasinski, P. Dixon, B. Hertzberg, A. Kvit, J. Ayala, G. Yushin, Nature Materials 9 (2010) 353–358.
[19] P. Kubiak, M. Pfanzelt, J. Geserick, U. Hörmann, N. Hüsing, U. Kaiser, M. Wohlfahrt-Mehrens, Journal of Power Sources 194 (2009) 1099–1598.
[20] Y.S. Hu, L. Kienle, Y.G. Guo, J. Maier, Advanced Materials 18 (2006) 1421–1426.
[21] K. Wang, M. Wei, M.A. Morris, H. Zhou, J.D. Holmes, Advanced Materials 19 (2007) 3016–3020.
[22] Y. Ren, L.J. Hardwick, P.G. Bruce, Angewandte Chemie International Edition 49 (2010) 2570–2574.
[23] D. Liu, Y. Zhang, P. Xiao, B.B. Garcia, Q. Zhang, X. Zhou, Y.H. Jeong, G. Cao, Electrochimica Acta 54 (2009) 6816–6820.
[24] D. Liu, G. Cao, Energy & Environmental Science 3 (2010) 1218–1237.
[25] Z. Hong, M. Wei, T. Lan, L. Jiang, G. Cao, Energy & Environmental Science 5 (2012) 5408–5413.
[26] Z. Hong, X. Zheng, X. Ding, L. Jiang, M. Wei, K. Wei, Energy & Environmental Science 4 (2011) 1886–1891.
[27] A.S. Barnard, P. Zapol, Physical Review B 70 (2004) 1–13.
[28] D. Wang, D. Choi, Z. Yang, V.V. Viswanathan, Z. Nie, C. Wang, Y. Song, J.-G. Zhang, J. Liu, Chemistry of Materials 20 (2008) 3435–3442.
[29] J. Liu, G. Cao, Z. Yang, D. Wang, D. Dubois, X. Zhou, G.L. Graff, L.R. Pederson, J.-G. Zhang, ChemSusChem 1 (2008) 676–697.
[30] H. Qiao, Y. Wang, L. Xiao, L. Zhang, Electrochemistry Communications 10 (2008) 1280–1283.
[31] J.S. Chen, X.W. Lou, Journal of Power Sources 195 (2010) 2905–2908.
[32] J. Jamnik, J. Maier, Physical Chemistry Chemical Physics 5 (2003) 5215–5220.
[33] P. Balaya, H. Li, L. Kienle, J. Maier, Advanced Functional Materials 13 (2003) 621–625.
[34] H. Furukawa, M. Hibino, I. Honma, Journal of the Electrochemical Society 151 (2004) A527–A531.

Zhensheng Hong received the B.S. degree (2008) in Department of Chemistry at Fuzhou University. He is now a Ph. D candidate at Fuzhou University. His research interests involve the synthesis of nanostructured materials for energy storage and conversion including lithium-ion batteries and dye-sensitized solar cells.

Mingdeng Wei received Ph.D degree in Catalysis Chemistry from Nagasaki University in 2000, and then worked at Tohoku University, National Institute of Advanced Industrial Science and Technology (AIST) and Japan Science and Technology Agency (JST). He is a Prof. at Fuzhou University from 2007 and his research interests include dye-sensitized solar cells, lithium-ion batteries and nanoporous materials.

Tongbin Lan obtained B.S. degree (2011) in Department of Chemistry at Fuzhou University. His current research involves the development of new type anode materials for lithium-ion batteries.

Guozhong Cao, Ph.D., is Boeing-Steiner Professor of Materials Science and Engineering and Adjunct Professor of Chemical and Mechanical Engineering at the University of Washington. He has published over 250 refereed papers, and authored and edited 5 books including "Nanostructures and Nanomaterials". His current research is focused mainly on nanomaterials for energy conversion and storage including solar cells, lithium-ion batteries, supercapacitors, and hydrogen storage materials.